Light-Triggered Association of Bovine Serum Albumin and Azobenzene-Modified Poly(acrylic acid) in Dilute and Semidilute Solutions

G. Pouliquen and C. Tribet*

Physico-chimie des Polymeres et Milieux Disperses, UMR 7615 CNRS & University Paris 6, ESPCI, 10 rue Vauquelin, F-75005 Paris, France

Received June 9, 2005; Revised Manuscript Received October 11, 2005

ABSTRACT: Reversible photoswitch of viscosity and photoresponsive binding of protein has been achieved in water solution of azobenzene-modified polyacrylate. We synthesized polymers with a few mol % hydrophobic side groups, including azobenzene groups with different spacers between the photochrome and the backbone. The binding of the protein (BSA) onto the polymers was investigated by capillary electrophoresis in dilute solution and rheology (viscosity, dynamic moduli, and stress relaxation) in semidilute solution of polymer. In the dilute regime, BSA/polymer complexes are formed in equilibrium with unbound BSA. Both the length of the hydrophobic spacer on the azobenzene side group and the presence of additional *n*-alkyl side groups significantly affect the affinity of BSA for the polymer. In the semidilute regime, viscosity enhancement by several decades is obtained upon addition of BSA in polymer solutions and ascribed to physical cross-linking involving BSA. In the two regimes, light was shown to modify the binding properties. Reversible release of BSA (by up to 80% of the protein) was obtained by exposure to UV. Reversible viscosity swings by up to 40-fold were cycled for hours by alternative exposure to UV/vis light. Light-induced cis−trans isomerization of the azobenzene together with low concentration of photochrome in the samples made it possible to obtain rapid responses (half-time ∼20 s) in solutions or in gels having thickness of the order of centimeters. An unprecedented degree of sensitivity is achieved thanks to the amplification provided by properties of optimal modified polymers. These properties are analyzed in term of the response of cross-links density, chain dynamics, and binding affinity.

Introduction

Amphiphilic macromolecules comprising both water-soluble and water-insoluble monomers form intrachain or interchain association in water. Noncovalent binding between hydrophobic moieties of the polymer provides the functional basis of applications including the replacement of high molecular weight viscosifiers[1] and dispersions of hydrophobic colloids including pigments, oil droplets, and proteins. The formation of large aggregates, even gels of interconnected hydrophobically modified polymers (HMPs), was recognized as common features of hydrophobically driven association between HMPs. Of practical importance are the possibilities to enhance and amplify the associating properties of HMP, in the presence of amphiphilic additives such as surfactant and proteins. Dramatic viscosifications and high sensitivity to external parameters are well-known and useful for applications using mixtures of HMP and surfactant's micelles.[2−4] For similar reasons, hydrophobic association between amphiphilic polymers and proteins have been proposed—and are actually used—in food as emulsifiers[5] and in biomedical applications such as proteins entrapment for protein stabilization, renaturation,[6,7] and drug delivery.[8−10] In concentrated solutions, HMPs such as alkyl-modified poly(acrylic acid) form highly viscous mixtures due to interchain hydrophobic association involving proteins.[11,12] This viscosification behavior reflects properties of the transient "cross-links" formed at the microscopic level. It has been proposed that a single protein can connect typically two polymer chains, with several hydrophobic side groups (less than ∼20) recruited in one "cross-link".[11] Other experiments performed in different conditions or with different polymers are also consistent with the binding of a few alkyl hydrophobes per protein: bovine serum albumin was found to form complexes at a ratio of hydrophobe/protein as low as ∼3:1, although in equilibrium with excess (unbound) protein;[13] telechelic HMP having exactly two hydrophobes per chain can form supra-macromolecular aggregates with the protein LPT1 bound to a single hydrophobic group of the polymer chain.[5]

We have endeavored to develop physical gels containing proteins, whose fluid−gel transition or entrapment/release of proteins can be tuned by the magnitude of hydrophobic binding involving proteins. To obtain versatile and rapid stimulation of the binding, even in highly viscous samples, we used light as a trigger of HMPs hydrophobicity. The hydrophobic side groups investigated (azobenzene photochromes) were accordingly rapidly and reversibly modified by light. Polymers having photochrome units in their hydrophobic moieties offer the unique opportunity to show reversible and specific variation of their properties with exposure to UV−vis light. Among photochrome groups that can be used, azobenzene groups have several advantages.[14] First, their light-triggered variation of polarity and conformation (cis−trans isomerization) do not depend on the polarity of the solvent and is readily obtained in water with excellent reversibility. Second, azobenzene dyes have been grafted on enzymes to trigger enzyme activity with light, and it was shown that the interaction between these dyes and the protein can depend on transconformations of the azobenzene groups.[15,16] In addition, photochrome-modified polymers have been designed to triggered variation of solution viscosity with light, although a rather limited magnitude of response was achieved (typically a few percent[17,18]). Those polymers show nevertheless significant change of their intrinsic viscosity, typically by a factor of 2, provided that the chain comprise a

* To whom correspondence should be addressed. E-mail: christophe.tribet@espci.fr.

10.1021/ma0512152 CCC: $33.50
Published on Web 12/09/2005

Scheme 1. (A) Chemical Structure of Photoresponsive HMP; (B) Chemical Structure of the Graft R: Azo or C12Azo and Its Isomerization under UV Exposure

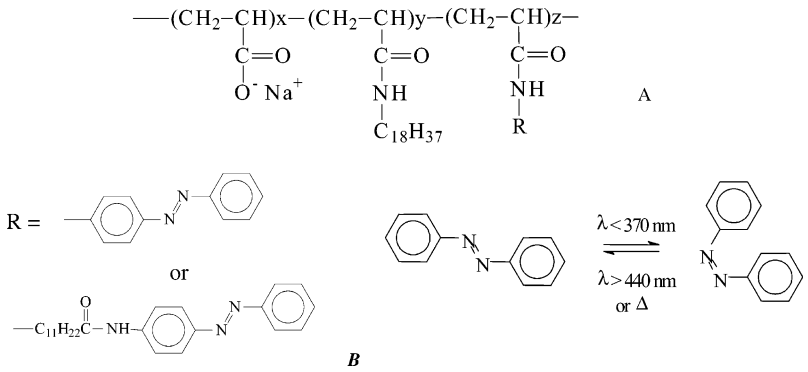

large fraction (above ~30−50 mol %) of photochrome monomers. The relatively high concentration of photochrome in samples and a limited magnitude of response were thus the key points to be improved for applications. Significant enhancement of the magnitude of response to light was recently obtained with conventional HMPs in combination with photochromic micelles.[19] Each micelle with ca. 50−100 azo-surfactant plays the role of a photoresponsive cross-link, which however levels up both the minimal chromophore concentration well above the critical micelle concentration and the chromophore/macromolecule ratio above ca. 100. Such a high chromophore content hampers unfortunately functioning at conditions of either short irradiation times (seconds or minutes) or weak photon fluxes (< mW/cm^2). There is indeed a major concern in centimeter-thick samples about photon absorption by the photochrome themselves. Low penetration of light in samples, solutions, or gels having millimolar concentration of photochrome dyes limits the stimulus to the top "skin" of the sample, within a thin layer of submillimeter thickness at these conditions (typical extinction coefficient of the photochrome is ca. 2×10^4 L mol^{-1} cm^{-1} at maximum absorption). Photochrome groups located deep inside centimeter-thick samples are thus hardly stimulated by light, except in the case of very efficient stirring. Homogeneous and complete response of thick samples requires accordingly hours-long irradiations.

Our strategy aims at achieving markedly higher sensitivity to light, affording the use of submillimolar, or even micromolar, concentrations of the photochrome. We combined light-responsive HMP/protein binding with light-responsive self-association of polymers. The advantages expected from this approach include (i) the versatility of tuning the viscosity/elasticity by simple mixing of protein and azobenzene-modified HMP, with no chemical modification required, and (ii) amplification of the response at both the stage of protein binding (specific recognition) and the stage of interpolymer (self-)-association. Because transient inter-HMP associations strongly modulate the macroscopic viscosity and elasticity, a few (critical) links in these physically cross-linked chains are expected to control the magnitude of viscosity enhancement. Extremely low concentration of cross-links matches well the requirement for low concentration of hydrophobic photochromes. Physical gelation and viscosity enhancement are in this framework ideally triggered by very limited modifications taking place on a few critical hydrophobic links. The nature of response to stimuli of these gels is expected to help better understanding of the structure and dynamics of hydrophobically driven gelation involving HMPs.

In this article, we present highly sensitive associations between the protein BSA and azobenzene-modified poly(acrylic acid) in water. We compared polymers of varying degree of modification and different spacers between the photochrome side groups and polymer backbone. In semidilute solution the formation of mixed aggregates was investigated by measurements of viscosity and elastic/loss moduli. Additional information on the binding was obtained in dilute solutions using a separation technique, capillary electrophoresis, to determine the fraction of bound and free BSA. We particularly focus on the comparison of the properties obtained in dark-adapted samples with that obtained under permanent exposure to UV or visible light. Finally, we propose a consensus model of polymer/protein association that can be used to account for the observed high sensitivity to light in all conditions.

Materials and Methods

Polymer Synthesis. HMPs were obtained by grafting a poly(acrylic acid) parent polymer (Polysciences Inc., Warrington, PA) having nominal MW 225 000 and 150 000 g/mol, respectively. Analysis by GPC of the poly(acrylic acid)s gave the corresponding weight-average molecular weights of 370 000 and 360 000 g/mol, with polydispersity indexes of 6 and 4, respectively (GPC was operated in 0.5 M $LiNO_3$, 40 °C, to avoid adsorption of poly(acrylic acid) on the column Shodex Ohpak SB-806 MHQ). A minor fraction of the acid groups were grafted in organic solvent by an octadecylamine and/or a primary amine containing the azobenzene group to yield the random copolymer shown in Scheme 1. The grafting procedure includes successive reactions of amines (octadecylamine and/or the azobenzene derivative) on the polyacid parent dissolved in *N*-methyl-2-pyrrolidone, in the presence of 1.2 equiv of dicyclohexylcarbodiimide as activating agent. Except where otherwise specified, all reagents were from Sigma-Aldrich and all solvents from SDS, France. After filtration of the reaction bath to remove the insoluble urea formed, the basic form of the polymer was obtained by neutralization with 1.5 equiv of sodium methanoate, which leads to polymer precipitation. Purification was achieved by three cycles of filtration, polymer dissolution in water (up to 10 wt %), and reprecipitation in methanol.[12,20] The grafted chromophores were either the aminophenylazobenzene (Aldrich, Milwaukee, WI) denoted "Azo" or the 12-aminoundecylamido-4-phenylazobenzene (i.e., azobenzene dye with a dodecyl "spacer") denoted C12Azo. The "C12Azo" amine was obtained from 12-aminododecanoic acid (Aldrich) by a three-step synthesis yielding (i) the "protected" amine with formation of urethane in the presence of excess di-*tert*-butyl dicarbonate in *tert*-butanol, (ii) coupling of aminophenylazobenzene and the protected compound in the presence of dicyclohexylcarbodiimide in ethyl acetate, and (iii) hydrolysis of the urethane in trifluoroacetic acid and dichloromethane. The designation of each polymer (Table 1 and Scheme 1) indicates the nominal MW of the parent polymer and the degree of grafting as determined by ^{1}H NMR (one peak from 1.8 to 2.2 ppm representative of 1 proton from the backbone, one peak at 3.0 ppm representative of side groups 2 methylene protons in the α-position of the amide function, and the 9 aromatic protons observed in the

Table 1. Composition of Azobenzene-Modified Polymers Determined by ^{1}H NMR and UV Spectrometry in Water

polymer	mol % octadecyl	mol % Azo	mol % C12Azo
150−1.2Azo	0	1.2 ± 0.1	0
150−4.5Azo	0	4.5 ± 0.3	0
150−1C18−0.5Azo	1.1 ± 0.1	0.5 ± 0.2	0
150−1C18−1.2Azo	0.9 ± 0.1	1.2 ± 0.1	0
150−1C18−4.5Azo	1.2 ± 0.2	4.5 ± 0.3	0
150−1C18−1C12Azo	1 ± 0.1	0	0.9 ± 0.2
225−1C12Azo	0	0	0.9 ± 0.1
225−2C12Azo	0	0	2 ± 0.1
225−3C12Azo	0	0	3.1 ± 0.1

range 7.0−7.8 ppm) and UV spectrometry (absorbance of the 4-amidoazobenzene moieties at 347 nm using the extinction coefficient 2.32×10^4 L mol^{-1} cm^{-1}).

Stock solutions of 2−4 wt % polymers in water were prepared under gentle stirring, for at least 24 h in the dark. To obtain samples for rheology, aliquots of a polymer stock solution were mixed with aliquots of a 10−100 g/L BSA (fraction V, Sigma-Aldrich) in water and stored at rest for 24 h. pH of the samples stabilized in the range 8.5−8.9, which corresponds to the preservation of almost complete ionization of the carboxyl group of the polymer. Prior to mixing, BSA solutions were filtered on 0.2 μm syringe filter (Millex, Millipore). To remove possible contaminant, some samples were prepared using dialyzed BSA solutions: BSA in borate buffer (see electrophoresis section) was dialyzed for 24 h against the run buffer (Slide-A-Lyzer MWCO 3500, Pierce). Electropherograms actually did not significantly differ while using dialyzed stock BSA or undialyzed BSA.

Viscosity Measurements. Viscosity measurements were performed using a Haake RS-150 rheometer (Rheo, France) equipped with a homemade PMMA transparent Couette cell.[21] The gap of this cell was 1 mm, with internal radius 15 mm; its external wall thickness was 0.1 mm, and its height was 15 mm. Cell calibration and parametrization for inertia compensation were achieved using standard siloxane oils (Brookfield Engineering lab., Stoughton, MA) in the ranges of viscosity 4.5−4800 cP and shear rate 0.1−500 s^{-1}. Above 100 cP, the observed viscosity appeared reliable and independent of shear rate (10−500 s^{-1}) within 5% uncertainty. Owing to the high transmission of light toward the external cell wall (>90% above 365 nm), it was possible to follow in situ the influence of the irradiation on the viscosity of samples. The measurements were performed at a constant shear rate (most typically 10 s^{-1}), ensuring the rapid and repeatable homogenization of the samples that were exposed on one side to an horizontal beam of light of diameter 75 mm, i.e., much larger than the cell, and having the same intensity as the beam used for ex-situ irradiations (cf. section Exposure to Light).

Dynamic Oscillatory Tests. Other rheological measurements (dynamic moduli and stress relaxation) were performed using a strain-controlled rheometer (Rheometrics Fluids spectrometer II Rheometrics, Inc, Piscataway, NJ) equipped with a plate−plate geometry and an upper transparent quartz plate of 40 mm diameter. Samples were slowly loaded onto the lower plate, and 10−15 min was allowed following gap adjustment, for the stresses to relax and for thermal equilibration (25 °C). The elastic modulus G' and the loss modulus G'' were obtained by subjecting samples to dynamic oscillatory tests during which a sinusoidal strain was applied, and the resulting stress was recorded at amplitude of strain of 20% and varying frequency in the range 0.01−100 rd/s. For stress relaxation experiments, an initial strain of 20% was applied in less than a millisecond and then maintained constant; stress was recorded for 1200−1500 s. Exposure to UV/vis light was provided by vertical irradiation from four optical fiber assemblies located a few centimeters above the upper plate on the four corners of a square, at a radius 15 mm from the rotation axis of the plate. The fibers were connected to the same irradiation device as described in Exposure to Light section.

Capillary Electrophoresis. Experiments were carried out with a Beckman P/ACE system MDQ instrument equipped with UV−vis detector (diode array multiwavelengths, Beckman Instruments, Fullerton, CA) operating in the range 4−8 kV and 25 °C. Bare silica capillaries of 75 μm × 31 cm and an effective length of 20 cm (J&W Scientific) were employed. The capillary was flushed daily with 0.1 M NaOH, followed by a water rinse, and finally was allowed to equilibrate with the run buffer (50 mM boric acid−NaOH, pH 9.2). Sample solutions were made from freshly prepared BSA solution and HMP solution both dissolved in run buffer. The concentration range of protein was 0.01−1 wt %, and polymer concentration was maintained constant at 0.01 or 0.02 wt %. Frontal analysis was carried out after at least a 2 h incubation of the samples, using continuous electrokinetic injection mode against the run buffer.[13]

Exposure to Light. Samples irradiations were carried out with a 350 W mercury arc lamp (Eurosep Instruments, France) combined with two quartz lenses affording to obtain a collimated horizontal beam of diameter ca. 75 mm. The beam was reflected onto a 45° mirror and passed through an ORIEL interference filter (365 or 436 ± 10 nm), before falling vertically into samples with a typical intensity of 1 mW/cm^2 at 365 nm. Samples were exposed to light for 10−30 min in a cooled water bath, prior to be analyzed rapidly in the dark, within less than 20 min after irradiation.

Results

Viscosity Enhancement in BSA/HMP Mixtures. We measured the viscosity of mixtures subjected to constant shear rate and prepared at a fixed polymer concentration, with the aim of identifying samples containing light-responsive clusters of polymer in solution. Viscosity was essentially used as a practical reporter sensitive to many behaviors including chain collapse or swelling, polymer binding to protein, and formation of transient network. In what follows, we discuss neither the structure of polymer clusters nor the relationship between interchain association and viscosity, both points being addressed in the section Viscoelastic Properties. Accordingly, we did not attempt to measure the zero-shear limit of viscosity: depending on samples, viscosity at shear rate 10 s^{-1} either corresponded to a shear-thinning region (most samples with BSA and C18 or C12Azo-modified polymers) or were close to the zero-shear limit for the more fluid samples (e.g., samples with no BSA and samples with BSA added to polymers 150−1.2Azo and 150−4.5Azo). The all-trans conformation of azobenzene groups was obtained by incubation for 24 h in the dark of samples prepared under visible light (i.e., with an initial minor fraction of *cis*-azobenzene of about 10 mol %; in the dark, this residual *cis*-azobenzene isomerizes slowly to form *trans*-azobenzene with a half-life time of ∼4 h).[22,23] The results shown in Figure 1A are typical for all polymers considered here in the concentration range 0.5−2 wt %. When polymers contain long alkyl side groups (C18 or C12Azo), an increase in BSA concentration sharply increases viscosity. In contrast, samples containing HMP with azobenzene groups closely grafted on the polymer backbone (150−1.2Azo, 150−4.5Azo, and 150−7Azo) show no significant variation of viscosity with BSA concentration, even at 2% polymer, i.e., the highest concentration used. Interestingly, the absence of viscosity enhancement in 150−1.2Azo, 150−4.5Azo, and solutions of the parent polymer with no hydrophobe (not shown, cf. ref 11) points to the negligible volume effect of the protein in samples and to the importance of interaction between BSA and long hydrophobes (C18 or C12Azo). The rise of viscosity in this concentration range (above the polymer $C^* \sim 0.2$ wt %) was ascribed in similar systems to the formation of HMP/BSA clusters by hydrophobic binding between the polymers chains.[11,24] Invariance of viscosity is accordingly a hint for the absence of—or very weak—associations.

When viscosity enhancement was observed, viscosity passed through a broad maximum at some optimal protein concentra-

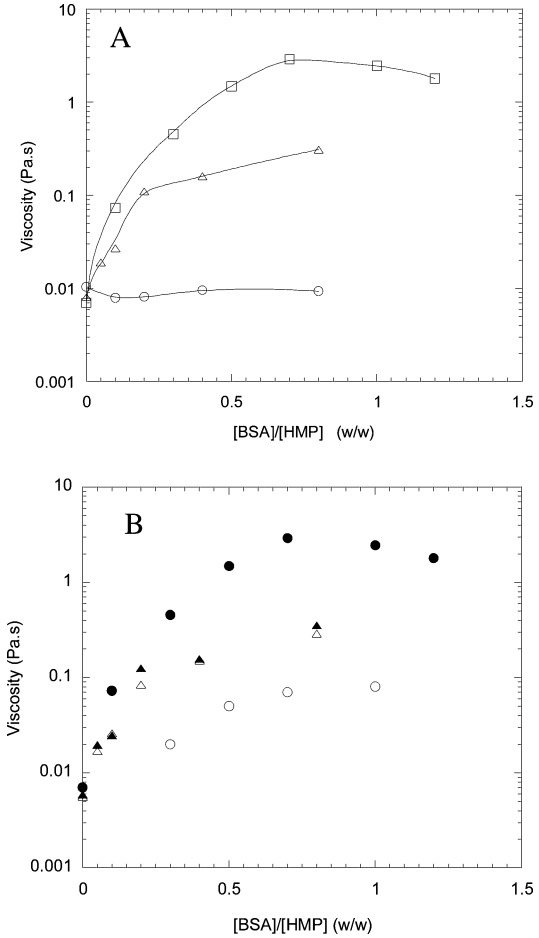

Figure 1. Viscosity of dark-adapted or UV-exposed HMP solutions in water at constant polymer concentration as a function of BSA concentration. Shear rate 10 s^{-1}. (A) Dark-adapted samples and (○) 2 wt % 150−4.5Azo, (△) 1 wt % 150−1C18−0.5Azo, and (□) 1 wt % 225−2C12Azo. (B) mixtures at 1 wt % polymer concentration in (closed symbols) dark-adapted samples or (open symbols) under exposure to UV light at 365 nm. (○, ●) 225−2C12Azo, (△, ▲) 150−1C18−0.5Azo.

tion. Corresponding compositions and viscosity are compared for different HMP in Table 2. The hydrophobe/BSA mol:mol ratio at this optimal compositions is found in the range 15−30. This ratio is remarkably larger than the number of hydrophobic sites on BSA (∼6).[25]

Viscosity can depend on whether the side groups are in all-trans (dark-adapted) or predominantly cis (UV-adapted) conformation. As shown in Figure 1B, dark-adapted samples containing 225−2C12Azo exhibited an increase in viscosity by up to 500-fold upon supplementation with BSA. At similar conditions, the optimal increase in UV-adapted samples did not exceed a factor of 10. The viscosity enhancement obtained in the presence of both BSA and UV light differed markedly for that obtained in the dark, provided that C12Azo groups are used (225−2C12 and 225−3C12). In contrast, solutions of HMPs with no spacer between the azobenzene and the backbone showed most typically very weak sensitivity to light, often close to the uncertainty of measurements (Figure 1B). The index $\varsigma = (\eta_{dark} - \eta_{UV})/\eta_{UV}$ (i.e., relative variation of viscosity) defines a magnitude of the effect of light, irrespective of differences between sample viscosities. Typical values of ς are given in Tables 2 and 3. The lowest values of ς, below 0.1 were obtained with copolymers modified with aminoazobenzene (i.e., no spacer: 150−1.2Azo, 150−4.5Azo). Error on viscosity measurement due to loading conditions (e.g., possible presence of small bubbles, effect of slow drying) was of similar amplitude. Samples of terpolymer comprising both C18 and azobenzene responded to UV irradiation with ς usually between 0.1 and 0.3, which was above uncertainty of measurements. Effects of similarly low magnitude have been reported for dilute solution of other azobenzene modified polymers.[27] This (low) magnitude of variation has been attributed to light-triggered changes in the extension of chains.[27] An index below 0.3 appears however negligibly small as compared to the viscosity swing obtained in optimized cases. Indeed, with polymer 150−1C18−4.5Azo containing a rather high density of azobenzene, the dark-adapted viscosity can be more than twice the viscosity obtained under UV exposure (Table 3). Exposure times longer than 10 min were however necessary to complete isomerization due to the high concentration of azobenzene in these samples. More rapid variations and even higher magnitudes were achieved upon exposure to UV of 225−2C12Azo and 225−3C12Azo solutions. Because of the lower concentration of dye in the latter samples, the cis isomerization is expected to occur more rapidly (cf. infra). The maximal variation of viscosity was obtained with 225−3C12Azo and reached a 40-fold drop (Tables 2 and 3). In the absence of BSA, with either polymer and at polymer concentration 0.4−1 wt %, the index ς was always below 0.1 (not shown). In samples of 225−1C12Azo, −2C12Azo, or −3C12Azo supplementation with BSA at concentration above ∼1 g/L was required to obtain significant response to light. In the range of compositions displaying a response to light, ζ did not change significantly with BSA concentration at fixed polymer concentration. Altogether, the results above rule out that possible change in chain conformation (possibly triggered by light) may have a significant role in the response of high magnitude. Although a mechanism cannot be discussed on the basis of the present viscosity experiments, the importance of hydrophobic binding between BSA and polymer makes no doubt. As regards interpretation of viscosity, information has to be collected from recording data at low shear rate. We recall here the shear-thinning behavior of samples in the range investigated and possible complex interplay between response to light and response to shear. For instance, in a sample containing 1 wt % 150−1C18−0.5Azo and 0.3 wt % BSA, a decrease in shear rate from 30 to 1 s^{-1} increased by 1.5-fold the magnitude of light-induced viscosity swings. While the present results clearly identify samples that can be triggered by light, the zero-shear limit of ζ would thus be more appropriate to compare those samples in term of their molecular response. Unfortunately, the design of the Couette cell required exposure to light on one side of the cell which hampers the use of very low shear rate due to homogeneity issues. Complete homogenization of samples requires a few rotations of the external cylinder of the cell. We observed that the rate of viscosity variation under exposure to light was slowed down by 2-fold while decreasing shear to 1 s^{-1}. Homogeneization would require several hours at shear rate compatible with a Newtonian behavior of the more viscous samples (<0.01 s^{-1}). At shear rate 10 s^{-1} (and above), the rate of light-triggered viscosity change was however invariant with shear rate and hence reflected an intrinsic kinetics of sample reorganization. For that reason, it was preferred obtain data at shear rate 10 s^{-1} and discuss first the rate of response to light and reversibility of the phenomena.

In-situ measurements of viscosity vs irradiation in a UV-transparent Couette cell show the reversibility and rapid kinetics of light-triggered fluidification of BSA/225−2C12Azo and BSA/225−3C12Azo samples (Figure 2). Results in Figure 2 are similar for other samples, with different magnitude of the

Table 2. Compositions of Samples and Their Viscosity Measured at Optimal Protein Concentration $[BSA]_{opt}$, Which Achieved Maximum Viscosity Enhancement for a Fixed HMP Concentration (Shear Rate 10 s^{-1})

polymers	150−4.5Azo	150−1C18−0.5Azo	225−2C12Azo	225−3C12Azo		150−3C18
concentration (wt %)	2%[d]	1%	1%	0.4%	0.7%	0.9%
maximal viscosity (Pa s)	0.01	∼0.35	2.9	1.3	5[c]	22[c]
$[BSA]_{opt}/[HMP]$ (g/g)	no	∼0.7	0.7 ± 0.1	1 ± 0.2	∼1	0.75 ± 0.3
$[hydrophobe]/[BSA]_{opt}$ (mol/mol)	no	∼15[a]	17 ± 3	20 ± 4	∼20	26 ± 9
ζ[b]	0.1	0.26	39	3	∼2[c]	no

[a] The [hydrophobe] stem from both azobenzene and octadecyl side groups. [b] Index $\zeta = \eta_{dark} - \eta_{UV}/\eta_{UV}$ is the magnitude of viscosity variation upon exposure to UV (365 nm) light. [c] Because samples were gellike, the value given is the dynamic viscosity obtained under oscillations at a frequency of 10 rd/s. "no" = no change of viscosity by more than the order of uncertainty. [d] Measurements at lower concentration were fraught with uncertainty because of the low viscosity achieved.

Table 3. Viscosity in the Dark and Magnitude of UV-induced Fluidification in BSA-HMP Mixtures

polymer	concn (wt %)	η_{dark} (mPa s)	ζ
150−1C18−0.5Azo	0.5	46	0.2
	1	1500	0.2
150−1C18−1.2Azo	0.5	41	0.5
	1	700	1.2
150−1C18−4.5Azo	0.5	100	0.3
	1	300	2.0
150−1C18−1C12Azo	0.5	380	1.5
	1	3600	0.2
225−2C12Azo	1	450	22
225−3C12Azo	0.4	220[b]	3
	0.7	5000[b]	2

[a] Shear rate 10 s^{-1} and 0.3 wt % BSA. ζ is defined in legend of Table 2 and was determined with typical experimental error of ±0.05. [b] Dynamic viscosity obtained from the dynamic moduli G' and G'' in gellike samples and 10 rd/s.

viscosity swing (ranging from 40-fold to almost zero). The highest viscosity is obtained in dark-adapted samples and shows a well-defined plateau value in absence of irradiation (Figure 2). Viscosity decreases immediately upon exposure to UV (365 nm) light. Recovery of part of the initial viscosity is obtained most typically within less than 100 s exposure to visible light (436 nm) and half recovery corresponding to less than 30 s irradiation. The viscosity drop (UV exposure) slowed down, however, with increasing polymer concentration, whereas viscosity recovery (under visible light) was not significantly affected by concentration. Samples were cycled for hours, several times between low and high viscosity states, with no apparent drift of their properties. In consistency with the latter hint for fair reversibility, the initial high viscosity was recovered after incubation for 24 h in the dark.

At similar conditions of exposure to visible light, but in dilute polymer solutions ([HMP] < 0.02 wt %), the rate of cis−trans isomerization of the photochrome was determined by spectrophotometry (half-time ∼19 s). It compares well to the rate of viscosity recovery. In contrast, the rate of trans−cis isomerization under UV light in dilute solution (half-time ∼26 s) appears significantly more rapid than the rate of viscosity drop (half-time ∼600 or ∼60 s in Figure 2). The rate of isomerization is, however, affected by high concentrations of photochromes and high UV absorbance of samples. When azobenzene concentration was above typically 10 mM, the kinetics of trans−cis transconformation was markedly slowed down as observed by spectrophotometry. In this regime, almost all UV photons are absorbed close to the surface of the samples, and the rate of isomerization decreases in bulk, which in turn causes the slowing down of viscosity variation. Viscosity swings of samples having the lowest concentration of photochrome were accordingly significantly more rapid (Figure 2B).

Viscoelastic Properties in the Dark. Viscosity is affected by both modifications of chain dynamics and chain connectivity, and we commented above on the limited range of shear rate

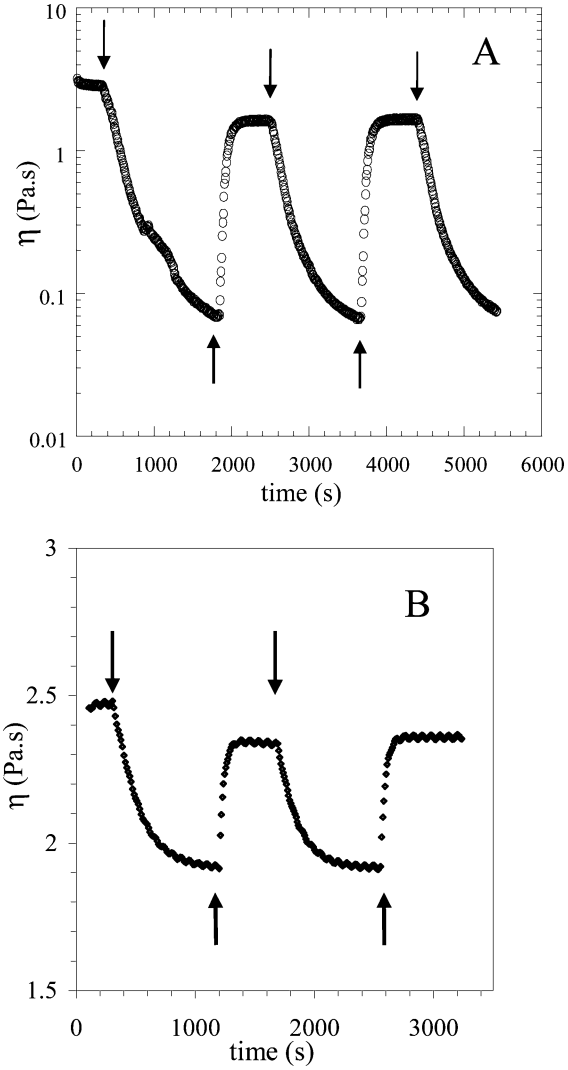

Figure 2. Variation of viscosity of 1 wt % HMP solution in the presence of BSA at constant shear rate (10 s^{-1}), under exposure to light with alternating the wavelength between UV (365 nm) and visible (436 nm). The times of wavelength switches are quoted by arrows in the figure. Initialy, the sample was equilibrated for 24 h in the dark (all-trans form) and first exposed to UV at time 400 s. (A) 225−2C12Azo and 0.7 wt % BSA; (B)150−1C18−05Azo and 0.6 wt % BSA.

investigated in the Couette cell. To address the question of whether cis−trans isomerization impacts interchain binding or interchain friction, we preferred to perform dynamic oscillatory tests and measurements of loss and elastic moduli. To characterize the mechanical properties of HMP aggregates, we measured frequency-dependent viscoelastic moduli with samples subjected to low strain amplitude (20%) in the range of linear viscoelastic response. A pseudo-plateau value in G' is clearly present in Figure 3A above 1 rd/s and representative of results obtained

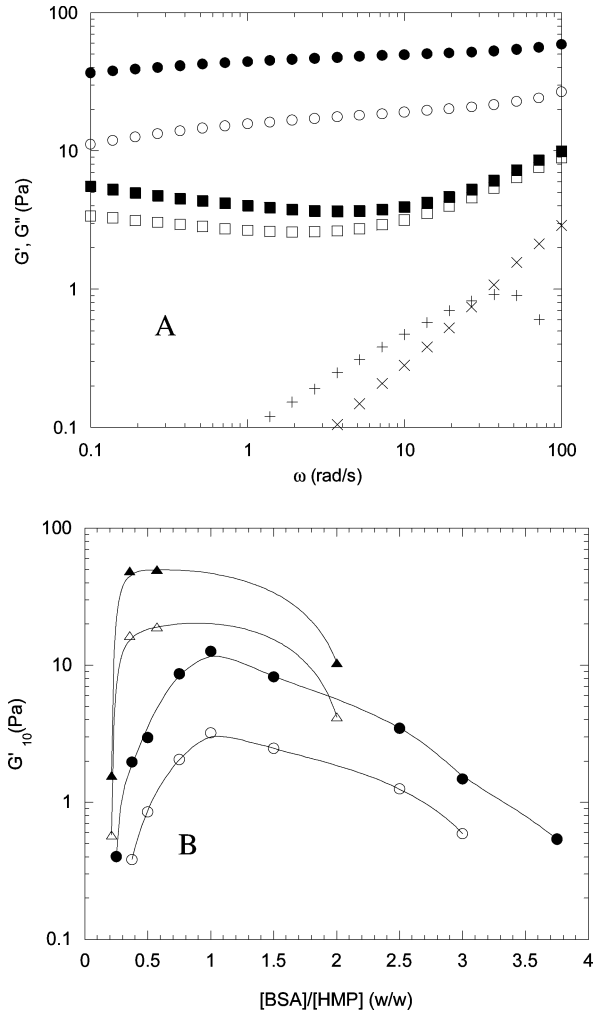

Figure 3. (A) Dynamic moduli of 0.7 wt % 225−3C12Azo in water with or without BSA. (○, ●) G' and (□, ■) G'' and 0.6% BSA; (×) G' and (+) G'' no protein. (B) Elastic modulus at 10 rd/s of BSA/225−3C12Azo mixtures at polymer concentration (○, ●) 0.4 wt % or (▲, △) 0.7 wt %. Closed symbols are for dark-adapted samples and open symbols for sample under exposure to UV light.

with samples containing BSA and 225−2C12Azo, or 225−3C12Azo as well, at polymer concentration >0.4 wt %. The dynamic response of these protein-containing samples was typical of physical gels and similar to results obtained in BSA/150−3C18 by Borrega et al.[11] G' reached a pseudo-rubbery plateau G_0 in the (high) frequency range. In contrast, solutions with no proteins showed markedly lower moduli and viscous character with $G'' > G'$ and $G'' \sim \omega$ in the experimental frequency window. Interestingly, the shear modulus obtained for samples with no BSA by using the Maxwell model extrapolation was 1−2 decades lower than the pseudo-rubbery plateau obtained in protein-containing samples. Because G_0 varies in proportion with the molar density of elastic strands, the number of HMP chains probed in absence of proteins appears to be negligible as compared to cross-link density formed in the presence of protein.

The value G'_{10} of G' at the fixed frequency 10 rd/s was reliably close to the value of the pseudo-rubbery plateau G_0 in most of the experimented window of BSA concentrations. The variations of G'_{10} with sample composition thus reflected changes in HMP connectivity. Figure 3B shows that the density of cross-links at constant polymer concentration can increase by decades with increasing BSA in dark-adapted samples. The maxima in connectivity of HMPs were obtained at protein/polymer ratios that were close to the maxima obtained by viscosity measurements described above (Table 2 and Figure 1). The corresponding samples contained HMPs/BSA complexes achieving optimal associating properties, at a protein:polymer w/w ratio of the order of 0.7−1 g/g. Another parameter reflecting the capacity to form interchain links is the quantity G_0/NkT (with N the number-concentration of chains). G_0/NkT varies by definition in proportion to the average number of elastically active strands per HMP chain and was in practice close to G'_{10}/NkT. In the polymer concentration window investigated, G'_{10}/NkT increased from virtually 0 up to 1.2 (using a MW of 370 000). Although the polydispersity issue may introduce a correction factor to N, and correspondingly affect the actual ratio of strand per chain, values of G'_{10}/NkT close to 1 point that a large fraction of HMP chains pertain to the elastic network. As expected, the highest values were reached in samples having the highest polymer concentration. Values going beyond 1.2 strands/chain would likely be obtained in more concentrated samples, above 1 wt % polymer. At optimal BSA/polymer ratio and at high HMP concentration, we obtain therefore that the density of strands can be larger than the density of HMP chains, and one HMP chain shall contain accordingly more than one cross-link.

The noncovalent and transient nature of inter-HMP bonds was investigated by stress relaxation experiments. Figure 4A shows that samples maintained at constant strain (20%) exhibit a slow decrease of stress, which can be fairly matched to a biexponential decay curve (eq 1). From fitting the parameters in eq 1, we obtained that the longer relaxation time τ_2 is the main relaxation mode (with $\beta > \alpha$). Within experimental uncertainty τ_2 was not sensitive to sample composition. In samples containing 225−3C12Azo, τ_2 was ca. 1400 ± 300 s (Figure 4B). Models of physical gels[28] predict that in the unentangled regime τ_2 is an estimate of the lifetime of clusters of HMPs.

$$G(t) = G_0[\alpha \exp(-t/\tau_1) + \beta \exp(-t/\tau_2)] \qquad (1)$$

with G_0 the relaxation modulus, τ_1 and τ_2 relaxation times, and α and β adjustable parameters in the range 0−1.

Viscoelastic Properties under Exposure to Light. Exposure to UV light decreased the value of G'_{10} and led to a drop in the pseudo-rubbery plateau of G' (Figure 3A,B), which was consistently attributed to a drop in inter-HMP cross-links. The density of chain associations clearly vanished upon cis isomerization of the azobenzene side groups. Within a set of samples prepared at fixed polymer concentration, the same relative variation (decrease) of G'_{10} upon exposure to UV was obtained irrespective of BSA concentration. In the log−log plot in Figure 3B, the effect of UV exposure on G' corresponds to an almost constant vertical shift as compared to dark-adapted samples. Interestingly, the dynamics of transient inter-HMP binding is not affected in the same way. Stress relaxation experiments performed under UV light showed similar decay rates that were essentially similar to those obtained with dark-adapted samples (Figure 4A). Analysis of the terminal time τ_2 with eq 1 provides accordingly constant values of τ_2 of the order 1400 s, irrespective of composition and irradiation (N.B.: though not shown, the same conclusion applies for the shorter time $\tau_1 \sim 80-100$ s). The main change achieved after UV exposure was a drop of the initial value of the relaxation modulus G_0 as illustrated in Figure 4A, in agreement with the decrease of the pseudo-rubbery plateau of G' obtained with dynamic oscillatory tests and with no significant change of chain dynamics.

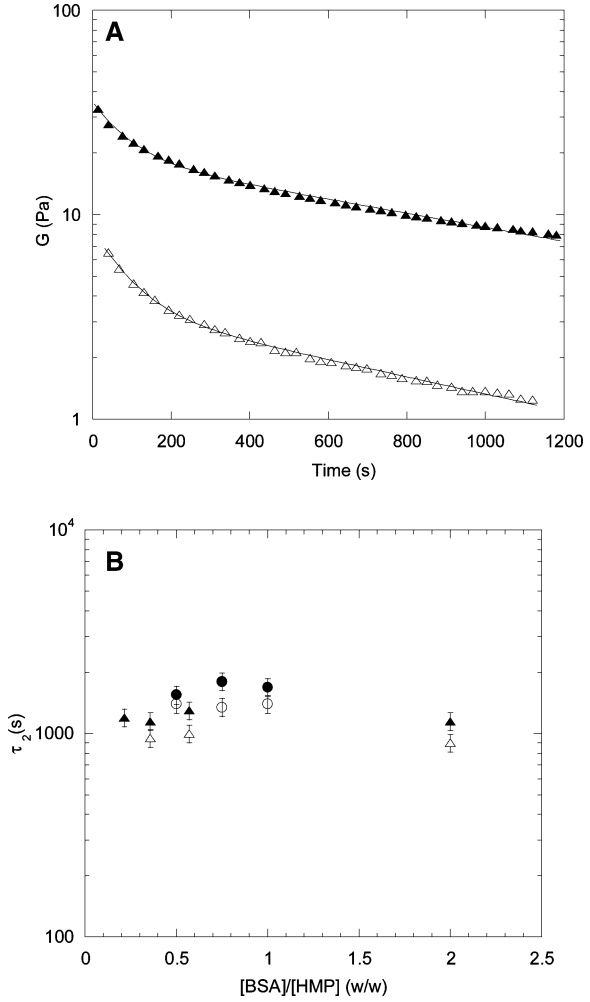

Figure 4. (A) Stress relaxation profile of a mixture of 0.7 wt % 225−3C12Azo and 0.25 wt %BSA. Lines are fit using eq 1. (B) Longest relaxation time vs BSA concentration as fitted to stress relaxation curves using eq 1. (△, ▲) 225−3C12Azo 0.4 wt %; (○, ●) 0.7 wt % 225−3C12Azo. Closed symbols are for dark-adapted samples and open symbols for sample permanently exposed to UV light.

Altogether, the results from the dynamic flow properties of 225−2C12Azo and 225−3C12Azo show that polymers form physical gels involving BSA in the cross-links. UV-irradiated polymers appear markedly less effective than dark-adapted polymers at forming interchain association in the presence of proteins, with UV-triggered transconformation causing in-situ breakage of most of the cross-links, irrespective of sample composition.

BSA Binding in Dilute Solutions. Protein/HMP binding was investigated in dilute solutions. Using an electrophoretic separation scheme now conventional in similar systems,[13,29] we can measure the concentration of free (unbound) BSA in equilibrium with BSA bound to HMP. Because of the lower charge/mass ratio of the free protein as compared to HMP and protein/HMP complexes, free BSA has an electrophoretic mobility smaller than all other species formed in the samples. At conditions of continuous injection of sample in the separation device, we obtained the formation of a sharp zone of free BSA (dragged out by the injection flow) preceding the zone of sample whose counterflow mobility slows down their motion (conditions of frontal analysis, see ref 13). UV-absorbance detection shows the separated zones, with first an increase corresponding to outflow of the free BSA, at time 2.4 min, followed by the short plateau of the zone containing free BSA (Figure 5). A second increase in absorbance is observed at time which depends on

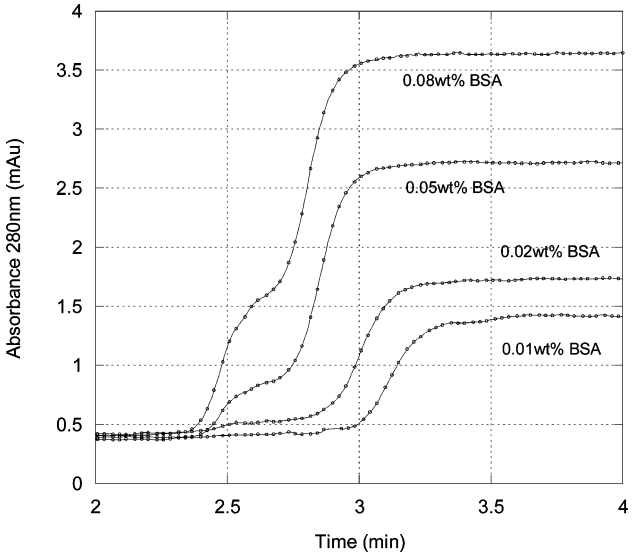

Figure 5. FACCE electropherograms of BSA/225−1C12Azo mixtures at polymer concentration of 0.01 wt % and varying protein concentrations as quoted in the figure. Samples were prepared 24 h before analysis (in 50 mM boric acid−NaOH buffer pH 9.2) and kept in dark to obtain the all-trans conformation of photochrome groups.

the outflow of HMP/BSA complexes (i.e., modulated by mobility of the complexes). With increasing concentration of BSA in samples, the electrophoretic mobility of the complexes is shown to decrease as reflected by the shift of their detection toward shorter times (3.1−2.7 min in Figure 5). The height of the first plateau in absorbance (determined at the inflection point on the electropherograms) varies in proportion with free BSA concentration $[BSA]_{free}$ and was calibrated using pure BSA standards. Binding isotherms as shown in Figure 6 can thus be calculated.

The initial slope on these isotherms appears dramatically sensitive to the type of azobenzene side group. A sharp initial increase with $[BSA]_{free}$ of the density of bound protein is observed for 225−1C12Azo and 3C12Azo polymers, below 10 μM $[BSA]_{free}$. The seemingly linear and comparatively smoother increase observed with 150−1.2Azo polymer continues up to 60−100 μM BSA_{free} (Figure 6A). In other words, the presence of a C12 spacer between the azobenzene group and polymer backbone enhances markedly the affinity of BSA for HMPs. Coulombic repulsions between the HMP polyanionic backbone and BSA (anionic at the basic pH used here) possibly restraint the accessibility of azobenzene with no spacer. The highest density of bound protein along the HMP chains was obtained at the highest concentration of free BSA with no clear damping off of the slope on the isotherms. For experimental reasons, it was not possible to obtain accurate data above a concentration of free BSA well beyond 100 μM, making it difficult to conclude about the saturation density of the chains. Nevertheless, the highest density measured with C12Azo HMPs corresponds to a ratio of azobenzene/BSA_{bound} approaching 1:1 (0.9:1 with 225−1C12Azo or 1.6:3 with 225−3C12Azo). In presence of excess free BSA, the density of bound protein on C12Azo-modified chains thus approaches a stoichiometry of one protein per azobenzene which should correspond to saturation. In contrast, the highest binding density measured with 150−1.2Azo levels off at ∼6:1 with an apparent saturation plateau above 60 μM BSA_{free}, a much larger apparent number of azobenzene per protein bound. Owing to the lowest affinity of BSA for 150−1.2Azo, it is likely that at this maximal density most of the azobenzenes are not bound on the protein.

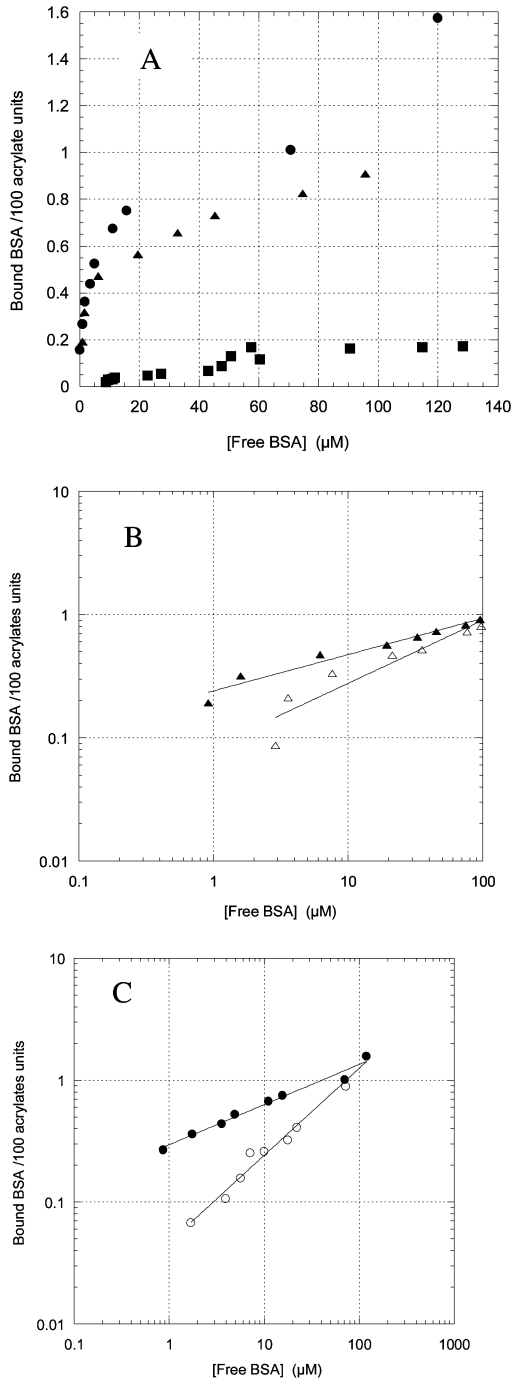

Figure 6. Binding isotherms of BSA on HMPs as obtained from FACCE analysis in 50 mM boric acid−NaOH buffer pH 9.2 and at polymer concentrations 0.01 and 0.02 wt %. (●) 225−3C12Azo, (▲) 225−1C12Azo, (■) 150−1.2Azo. (A) Dark-adapted samples kept 24 h and analyzed in absence of light. (B, C) Log−log plot of isotherms obtained with (closed symbols) dark-adapted samples or (open symbols) after exposure to UV light for 10 min. (▲, △) 225−1C12Azo; (●, ○) 225−3C12Azo.

Exposure to UV light causes at least partial dissociation of the complexes formed in the dark, as shown in Figure 6B,C. The release of part of the bound protein was reliably obtained with all polymer tested. On the binding isotherm, this light-triggered release depends, however, on the concentration of free BSA. The magnitude of the UV-triggered downshift of the binding density (Figure 6B,C) is clearly more important at low $[BSA]_{free}$, when almost all the protein added in samples are trapped in HMP chain in the dark. More than 80% of the BSA can for instance detach from 225 to 3C12 upon irradiation, at conditions which correspond to an initial association density below 4BSA/1000 monomers. Interestingly, the ratio of azobenzene/protein at condition of this efficiency of release corresponds here to ca. 10−15 Azo groups per BSA bound, which compares well with the optimal ratio used above to prepare the physical gels.

Discussion

Reversible variation upon exposure to UV, of both sample viscosity (or G') and BSA binding on HPMs, point to marked differences in protein affinity for *cis*- and *trans*-azobenzene, respectively. Some samples, however, showed no response to light despite BSA is bound on the polymer. The goal of the discussion is to interpret these results in order to propose a model of HMPs and HMP/BSA associations involving the azobenzene hydrophobes and accounting for specificity due to the polymer nature of the photochromes. First, we assume in the following that BSA keeps its globular folding and a nativelike state in all the samples, irrespective of binding to HMPs. Preservation of the secondary structure of the protein was established in similar HMPs/BSA gels[11] by measurements of optical rotation. The optical rotatory dispersion (ORD) of BSA solutions did not change upon supplementation with 150−1C18−1.2Azo and was not affected by UV exposure. Denaturation leads most often to changes in ORD, irreversible aggregation, and turbidity. None of these phenomena were observed in our samples. In addition, samples showed no drift of viscosity with incubation under shear, and excellent reversibility of light-triggered swings, which points to a fairly stable state of BSA dispersed in solution.

Gel Structure and Interchain vs Intrachain Association. This paragraph focuses on polymers capable of gellike behaviors and high-viscosity enhancement in the presence of BSA (e.g., 225−*x*C12Azo, 150−1C18−1Azo). Other systems with weaker variations of viscosity presumably form BSA/HMP clusters, though commenting on their properties needs other investigations but rheology. The parameters required for a description of the microstructure of the physical gels would ideally include the length and density of elastically active strands, the density of BSA bound along the chains, the fraction of protein involved in cross-links, functionality, and lifetime of cross-links. Some of these parameters can be inferred from the present data.

We first consider how binding isotherms constrain the binding in dark-adapted gels. The isotherms of Figure 6 reflect equilibrium states in the dilute regime that were found independent of the dilution of HMPs chains (ref 13 and unpublished data on azo-modified chains). It is reasonable to assume that the same binding isotherms still apply at higher polymer concentration, close to the transition toward semidilute regime, until interchain contacts are not predominant. At the conditions of optimal associating properties identified above as HMP:BSA ∼ 1 g/g, the molar ratio between BSA and acrylic monomers is about 0.15 mol %. On the isotherms in Figure 6B, 0.15 BSA molecules bound per 100 monomers corresponds to a concentration of unbound protein below 8 and 2 μM, respectively (i.e., below 0.6 and 0.13 g/L). The expected concentration of unbound protein is therefore much lower than the concentration of bound protein and becomes smaller with increasing polymer concentration (total BSA = 4−10 g/L in samples showing the optimal associating properties). Similar estimates can be made for other compositions of the gels and show that the fraction of unbound proteins is essentially negligible in most of the experimental window, even in samples prepared at high BSA content ($[BSA]_{total}$/[HMP] > 3−4 g/g). The density of bound BSA and a corresponding average number of monomer between two

proteins successively bound along the chain are now readily estimated from the ratio of the total number of protein to the number of HMP monomers in sample. Because some samples contained just a few BSA per HMP chain, eq 2 accounts for dangling chain ends by assuming that the average length of both end-segments equals half the distance between two BSA in the chain:

$$L_{\mathrm{BSA-BSA}} = \langle L\rangle/(B+1) \approx \frac{1}{M_{\mathrm{mono}}([\mathrm{BSA}]_{\mathrm{tot}}/M_{\mathrm{BSA}}[\mathrm{HMP}] + 1/\mathrm{MW})} \quad (2)$$

where $\langle L\rangle = \mathrm{MW}/M_{\mathrm{mono}}$ is the average number of monomers per HMP chains, MW, M_{BSA}, and M_{mono} are the molecular weight of HMP, BSA, and a monomer of HMP, respectively, [HMP] is the concentration by weight of HMP, $[\mathrm{BSA}]_{\mathrm{tot}}$ is the weight concentration of protein added in the sample, and B is the number of bound BSA per chain which writes if one neglects $[\mathrm{BSA}]_{\mathrm{free}}$: $B \approx [\mathrm{BSA}]_{\mathrm{tot}}/M_{\mathrm{BSA}} \times \mathrm{MW}/[\mathrm{HMP}]$.

With a polymer length equal to a few thousand monomers (typically 4000) and a weight ratio of protein/HMP of 0.7−1 g/g at optimal associating properties, $L_{\mathrm{BSA-BSA}}$ is calculed from eq 2, giving most typically $L_{\mathrm{BSA-BSA}} = 570$ and $N \sim 6$ protein per chain. On the other hand, the average length of an elastically active strand, L_{st}, is calculated using the number of strands per chain, $N_{\mathrm{st}} = G_0/NkT$ (see result section Viscoelastic Properties in the Dark) in eq 3 accounting for dangling ends at both ends of the chains. In samples showing the highest modulus G_0, L_{st} takes a value of 1900 monomers and $N_{\mathrm{st}} \sim 1$. Comparing L_{st} and $L_{\mathrm{BSA-BSA}}$ suggests that a maximum of one-third to one-fourth of all the bound BSA is actually involved in cross-links in ∼1 wt % HMP solutions. Intrachain binding rapidly prevails over interchain cross-links in samples that are either more dilute or suboptimal in terms of BSA/HMP ratio.

$$L_{\mathrm{st}} = \frac{\langle L\rangle}{(N_{\mathrm{st}}+1)} = \frac{1}{M_{\mathrm{mono}}\left(\frac{G_0}{kT[\mathrm{HMP}]} + 1/\mathrm{MW}\right)} \quad (3)$$

with N_{st} the number of strands per HMP chain, G_0 the pseudo-rubbery plateau modulus, k the Boltzmann constant, and T the temperature.

When interchain binding is strong enough, it is expected that the conformational motion of elastic strands is significantly more rapid than cross-link dissociation. In consistency with that expectation, the crossover frequency of G' and G'' shifts dramatically from 40 rd/s toward frequencies below 0.1 rd/s, upon supplementation of HMP solutions with little BSA content (protein/HMP above to 0.1 g/g). This shift suggests that HMP clusters formed in the presence of the protein survive for a time much longer than the time required for unbound HMP chains to explore their available conformational space. At such conditions, the terminal time measured by stress relaxation (∼1500 s) should provide information on the lifetime of cross-links. Long relaxation time τ_2 of the order of 1 h points to a rather long persistence of the network structure. Long lasting of the network does not, however, imply long lifetime of cross-links because connectivity and polyelectrolyte effects can constrain the motion of strands which dissociate and reassociate many times at the same place before a significant change of network conformation is obtained.[28] The unexpected behavior in our sample is rather the invariance of the terminal time with connectivity as modulated by BSA concentration or under exposure to light. Sticky reptation models[30] and Rubinstein and Semenov's models[28] both predict important slowing down of the chain dynamics while increasing the average number density of interchain binding. The experimental invariance of relaxation rate (both rapid and slow relaxation modes) with G_0 points in contrast to a remarkably constant lifetime of the critical strands. Assuming that elastically active strands are formed by a subpart of an HMP chain bridging two cross-links, the lifetime of a strand can accordingly be invariant. We propose that in the concentration range investigated the polydispersity of HMP chains may broaden the conditions of prevalence of single-HMP strands, a point which is not addressed in theoretical approaches: In polydisperse polymers, the elastic strands formed by the longest chains could predominate at low BSA concentration, i.e., low density of cross-links; the contribution of shorter chains would become significant when the density of BSA bound per chain increases, because shorter polymers have to bear enough protein (at least 2 per chain) to participate in a network. The corresponding regular decrease of the length of the elastic strands with increase in G_0 at fixed polymer concentration is thus accompanied by a similar decrease of the average length of the HMP chains recruited in the network.

Light-Triggered Affinity between HMP and Protein. The ability of the dark-adapted chain to bind BSA depends on azobenzene accessibility and is sensitive to the presence of C12 spacer between the chain and the chromophore groups. Coulombic repulsion affect the interaction (both partners are anionic), but it should not be significantly modified by the length of azobenzene side groups. It is thus likely that the improvement of binding observed using the C12 spacer comes essentially from changes in steric and hydrophobic effects. An increased versatility in conformations using C12 spacer should give better matching with binding sites. An increased hydrophobicity due to the alkyl nature of the spacer may balance Coulombic repulsion. Binding isotherms of C12Azo-modified chains compares in the dark with C18-modified chains of similar modification degree,[13] which agrees with a marked hydrophobic contribution of the aromatic part. As regards the effect of light, binding isotherms show that *trans*-azobenzene side groups have most typically a higher affinity for BSA than the corresponding cis isomers. It is tempting to propose that the effect of light could be captured by an effective decrease in hydrophobicity of the side groups. The properties of (trans)C12Azo, almost similar to *n*-octadecyl group, would simply turn into another equivalent alkyl group shorter than C18. Binding isotherms to *n*-alkyl-modified HMPs show, however, high anticooperativity, with slope ∼1/3 in log plots of the isotherms.[13,31] Preservation of anticooperative behavior, irrespective of *n*-alkyl length and grafting density, contrasts with the noncooperative binding obtained with the predominantly cis 225−3C12Azo under UV exposure (Figure 6C). This makes it difficult to propose simple equivalent short alkyl groups that may compare with *cis*-azobenzene groups. Anticooperativity corresponds to an effective energy loss upon increasing the density of bound BSA, i.e., apparent repulsion between bound proteins. Under exposure to UV, noncooperative binding emerges, at least at low $\mathrm{BSA}_{\mathrm{free}}$. Binding to (cis) azobenzene is certainly much weaker than to the (trans) group, but in addition isomerization appears to cancel totally the apparent intrachain BSA−BSA repulsions. Differences in protein orientation upon binding to cis groups can possibly change protein−protein interaction. Alternatively, intrachain azobenzene−azobenzene or alkyl−alkyl hydrophobic association can also compete with the binding of BSA and modulate the free energy of binding in complicated ways. It would be premature to settle here, which origin among the

several possibilities explains changes in cooperativity. We ascribe the UV-triggered release to both a modification of azobenzene affinity for BSA and to profound modifications of the intra-HMP interactions between monomers and proteins. Investigation on intra-complex interaction remains an open question that may possibly bring some optimization of the present systems in term of magnitude of response to UV. A large matrix of parameters is still available, including the effect of spacer length and density, HMP ionization degree (pH), ionic strength, etc.

At low concentration of free BSA, exposure to UV leads to a release of most of the protein bound as judged from binding isotherms (more than 75% below 7 μM BSA_{free} and up to 80% obtained in the case of 225−3C12Azo). If dissociation of inter-HMP cross-links takes place to a similar degree, almost complete vanishment of the physical gel is expected since the elastic strands are typically single HMP chains bound to a limited number of interchains links. At these conditions, only the longest chains among the polydisperse mixture of chains may keep the capacity to form a network. The drop by $\times$40 of either viscosity or shear modulus upon UV exposure is consistent with this high extent of disconnection (Figure 2). But it was also found "only" $\times$4 with 225−3C12Azo in the whole experimental window (Figure 3). The dissociation of cross-links seems in the latter case smaller than expected. In concentrated solutions of polymers, the release of BSA appears, however, buffered by the equilibrium with HMP chains. At variance with the dilute regime, the concentration of unbound protein indeed increases significantly upon release of bound protein, which in turn affects the equilibrium density of BSA bound. It appears that light-induced change in $[BSA]_{free}$ can at these conditions balance the light-triggered decrease in affinity. On the typical example of a 0.7 wt % 225−3C12Azo containing ~0.3 BSA/100 monomers in the dark ($[BSA]_{free} \sim 1$ μM), a 30% release lead to increasing $[BSA]_{free}$ by ca. 6−7 μM, which reaches the equilibrium value corresponding to 0.21 BSA bound/100 monomer under light-exposed conditions (Figure 6C). Because of the increase in concentration of unbound BSA upon release from HMP, the density of bound protein does not decrease by a factor of 5−10 as obtained in dilute regime but is expected to level off at −30%. In this framework, the decrease by a factor of 4 of the connectivity obtained in 225−3C12Azo samples contrasts with the expected −30% drop in binding density. Moreover, the light-triggered disconnection was almost independent of the concentration of BSA, which also points to differences between the behavior of cross-links and the association of BSA to isolated chains. We conclude that cross-links dissociation by UV light is essentially not sensitive to concentration of free protein. The binding of BSA to several HMP chains clearly shows different behavior than binding onto an isolated chain but clearly is highly sensitive to light, too. These features are pictured in Figure 7.

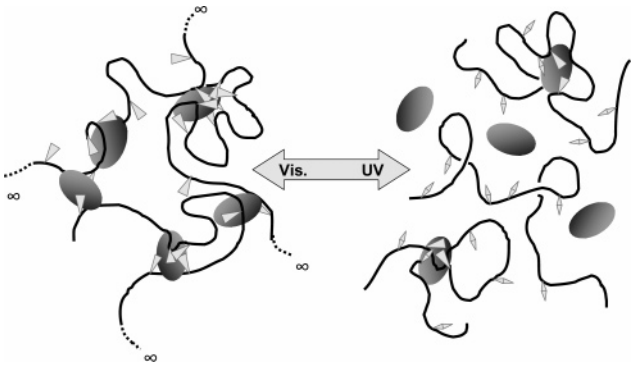

Figure 7. Sketch of light-triggered binding of proteins on HMPs. Proteins mostly bound under exposure to visible light show significant release under UV exposure, with an even more extensive breakage of cross-links. For clarity of the picture, the number of protein represented in intrachain binding is more than 4-fold below experimental estimates and the side groups of HMPs are oversized. *trans*-Azobenzene side groups are drawn as triangles, and their cis form appears as mostly unbound lozenges.

Conclusion

Putting together the results converges to give a consistent picture of HMPs dilute solution, semidilute network, and the influence of light on both gel connectivity and BSA binding/release. Rapid equilibration ($\ll$1 min) between free BSA and bound ones is shifted toward tighter association by either the presence of long alkyl side groups, an hydrophobic spacer, or cis-to-trans isomerization. At their maximum capacity HMPs bind up to one BSA per ~1 azobenzene group, which corresponds to typical BSA/HMP weight ratio of ~5−30 g/g using polymers of low modification rate (1−5 mol %). In gellike samples prepared below 2% HMP (~10C^*), the elastically active strands comprise more or less one HMP chains and several BSA bound. High viscosity and elastic properties are obtained well below saturation of HMPs, at protein/polymer ratio below ~3 g/g. Most of the proteins are bound in dark-adapted gels, though most do not form cross-links. Exposure to light disrupts rapidly (< seconds) the interchain bonds and simultaneously causes the release of BSA in solution. The sensitivity of BSA release to concentration of free protein indicates that the cis form of azobenzene has some affinity for BSA, a point supported by similar binding density of BSA on HMPs irrespective of light exposure, in the presence of large excess of free protein. In contrast, the degree of cross-link disruption by light appears essentially invariant with both the concentration of unbound BSA and the density of bound BSA. This observation suggests that the stability of cross-links is controlled mostly by structural parameters such as the accessibility of side groups and the distance along the chains between azobenzene. In addition, similar invariance of the network relaxation rate with either exposure to light or BSA concentration suggests a structure of cross-links essentially unmodified by both the presence of *cis*-azobenzene and the degree of BSA bound. It appears most likely that a relatively well-defined composition of the cross-links gathering several trans isomers and one BSA is formed.

In comparison with previous photoviscosity coupling based on chain extension or binding to photochrome micelles,[16−18] the present approach achieve high magnitude of response (3−40-fold variation) at significantly lower concentration of chromophores (0.2−4 mM). This efficiency is likely to be due to good recruitment of the photochromes in the physical cross-links, together with high sensitivity of cross-linking to isomerization. Because concentration above a few millimolar decreases considerably the rate of isomerization in bulk, it might be useful to further decrease the photochrome content. In the present examples, a ratio of 10−20 azobenzene groups per protein was needed to obtain optimal associating properties. These compositions were above the minimum ratio expected to preserve the capacity of light-sensitive cross-linking, i.e., a diminishing down to 1−2 azobenzene per BSA. Our results tend to suggests that polymer composition control the structure and response of cross-links, irrespective of both sample concentration and fraction of BSA bound. Saving one more decade in the absorbance of sample appears therefore still possible by optimizing polymer composition. Increasing the distance to C^* may also favor inter-HMP assemblies with lower azobenzene engaged in intrachain links with BSA.

Finally, the principle of using colloids to enhance interchain binding is not limited to proteins and can be readily generalized to other additives having the capacity to form physical cross-links with photochrome-containing HMPs. We are currently investigating the properties of micelles of conventional surfactants and cyclodextrin−polymers as alternatives to BSA.

Acknowledgment. We thank particularly C. Prata for help in the synthesis of the C12 spacer and Ph Sergot and G. Ducouret for development of the transparent Couette cell. G. Pouliquen's PhD was granted by the french MRT. We acknowledge support from ACI "physico-chimie de la matiere complexe" no. PC54-01.

References and Notes

(1) Goddard, E. D.; Ananthabadmanabhan, K. P. *Surf. Sci. Ser*. **1998**, *77*, 22−64.
(2) Picullel, L.; Thuresson, K.; Ericsson, O. *Faraday Discuss.* **1995**, *101*, 307−318.
(3) Furuya, T.; Koga, T.; Tanaka, F. *J. Polym. Sci., Part B* **2004**, *42*, 733−751.
(4) Panmai, S.; Prudhomme, R. K.; Peiffer, D. *Colloids Surf.* **1999**, *147*, 3−15.
(5) Renan, M.; Francois, J.; Marion, D.; Axelos, M.; Douliez, J.-P. *Colloids Surf., B* **2003**, *32*, 213−221.
(6) Tribet, C.; Audebert, R.; Popot, J.-L. *Proc. Natl. Acad. Sci. U.S.A.* **1996**, *93*, 15047−15050.
(7) Akiyoshi, K.; Sasaki, Y.; Sunamoto, J. *Bioconjugate Chem.* **1999**, *10*, 321−324.
(8) Akiyoshi, K.; Kobayashi, S.; Shichibe, S.; Mix, D.; Baudys, M.; Kim, S. W.; Sunamoto, J. *J. Controlled Release* **1998**, *54*, 313−320.
(9) Constancis, A.; Meyrueix, R.; Bryson, N.; Huille, S.; Grosselin, J.-M.; Gulik-Krzywicki, T.; Soula, G. *J. Colloid Interface Sci.* **1999**, *217*, 357−368.
(10) Lukyanov, A. N.; Torchilin, V. P. *Adv. Drug Delivery Rev.* **2004**, *56*, 1273−1289.
(11) Borrega, R.; Tribet, C.; Audebert, R. *Macromolecules* **1999**, *32*, 7798−7806.
(12) Pouliquen, G.; Porcar, I.; Tribet, C.; Amiel, C. *Polymer Gels: Fundamentals and Applications*; *ACS Symp. Ser*. **2003**, *833*, 262−289, Chapter 18.
(13) Porcar, I.; Cottet, H.; Gareil, P.; Tribet, C. *Macromolecules* **1999**, *32*, 3922−3929.
(14) Rau, H. Azo Compounds. In *Photochromism Molecules and Systems*; Dürr, H., Bouas-laurent, H., Eds.; Elsevier: Amsterdam, 2003; pp 165−190.
(15) Willner, I.; Rubin, S.; Shatzmiller, R.; Zor, T. *J. Am. Chem. Soc.* **1993**, *115*, 8690−8694.
(16) Lee, C. T.; Smith, K. A.; Hatton, T. A. *Biochemistry* **2005**, *44*, 524−536.
(17) Irie, M.; Hirano, Y.; Hashimoto, S.; Hayashi, K. *Macromolecules* **1981**, *14*, 262−267.
(18) Moniruzzaman, M.; Sabey, C. J.; Fernando, G. *Macromolecules* **2004**, *37*, 2572−2577 and references therein.
(19) Lee, C. T.; Smith, K. A.; Hatton, T. A. *Macromolecules* **2004**, *37*, 5397−5405.
(20) Wang, T. K.; Iliopoulos, I.; Audebert, R. *Polym. Bull. (Berlin)* **1988**, *20*, 577−589.
(21) Porcar, I.; Sergot, P.; Tribet, C. In *Stimuli Responsive Water Soluble & Amphiphilic Polymers*; *ACS Symp. Ser.* **2001**, *780*, 82−100, Chapter 5.
(22) Porcar, I.; Perrin, P.; Tribet, C. *Langmuir* **2001**, *17*, 6905−6909.
(23) Morishima, Y.; Tsuji, M.; Kamashi, M.; Hatada, K. *Macromolecules* **1992**, *25*, 4406−4410.
(24) Petit, F.; Audebert, R.; Iliopoulos, I. *Colloid Polym. Sci.* **1995**, *273*, 777−779.
(25) Peters, T., Jr. *All about Albumin. Biochemistry Genetics and Medical Applications;* Academic Press: New York, 1996; Chapters 2−3, pp 54−131.
(26) Tribet, C.; Porcar, I.; Bonnefont, P. A.; Audebert, R. *J. Phys. Chem. B* **1998**, *102*, 1327−1333.
(27) Irie, M.; Schnabel, W. *Macromolecules* **1985**, *18*, 394−398.
(28) Rubinstein, M.; Semenov, A. *Macromolecules* **1998**, *31*, 1386−1397.
(29) Gao, J. Y.; Dubin, P. L.; Muhoberac, B. B. *Anal. Chem.* **1997**, *69*, 2945−2949.
(30) Leibler, L.; Rubinstein, M.; Colby, R. *Macromolecules* **1991**, *24*, 4701−4709.
(31) Tribet, C. *Surfactant Sci. Ser*. **2000**, 687−741, Chapter 19.

MA0512152